# Studies of interaction of homo-dimeric ferredoxin-NAD(P)+ oxidoreductases of Bacillus subtilis and Rhodopseudomonas palustris, that are closely related to thioredoxin reductases in amino acid sequence, with ferredoxins and pyridine nucleotide coenzymes



doi: 10.1016/j.bbapap.2008.12.014

**Title**:

Studies of interaction of homo-dimeric ferredoxin-NAD(P)$^+$ oxidoreductases of *Bacillus subtilis* and *Rhodopseudomonas palustris,* that are closely related to thioredoxin reductases in amino acid sequence, with ferredoxins and pyridine nucleotide coenzymes

**Authors**:

Daisuke Seo, Seisuke Okabe, Mitsuhiro Yanase, Kunishige Kataoka and Takeshi Sakurai

**Address**

Division of Material Sciences, Graduate School of Natural Science and Technology, Kanazawa University, Kakuma, Kanazawa, Ishikawa 920-1192, Japan

**Type of Paper**

Regular paper

**Short title**

Ferredoxin:NADP$^+$ oxidoreductases of *Bacillus* and *Rhodopseudomonas*

**Corresponding author**: Daisuke Seo

Division of Material Sciences, Graduate School of Natural Science and Technology, Kanazawa University, Kakuma, Kanazawa, Ishikawa 920-1192, Japan

Telephone: +81-76-264-5683

Fax number: +81-76-264-5742

e-mail: dseo@cacheibm.s.kanazawa-u.ac.jp

**Keywords:** ferredoxin, ferredoxin-NADP$^+$ oxidoreductase, firmicutes, green sulfur bacteria, FNR

**Abstract**

Ferredoxin-$NADP^+$ oxidoreductases (FNRs) of *Bacillus subtilis* (YumC) and *Rhodopseudomonas palustris* CGA009 (RPA3954) belong to a novel homo-dimeric type of FNR with high amino acid sequence homology to NADPH-thioredoxin reductases. These FNRs were purified from expression constructs in *Eschelichia coli* cells, and their steady-state reactions with [2Fe-2S] type ferredoxins (Fds) from spinach and *R. palustris*, [4Fe-4S] type Fd from *B. subtilis*, $NAD(P)^+$/NAD(P)H and ferricyanide were studied. From the $K_m$ and $k_{cat}$ values for the diaphorase activity with ferricyanide, it is demonstrated that both FNRs are far more specific for NADPH than for NADH. The UV-visible spectral changes induced by $NADP^+$ and *B. subtilis* Fd indicated that both FNRs form a ternary complex with $NADP^+$ and Fd, and that each of the two ligands decrease the affinities of the others. The steady-state kinetics of NADPH-cytochrome *c* reduction activity of YumC is consistent with formation of a ternary complex of NADPH and Fd during catalysis. These results indicate that despite their low sequence homology to other FNRs, these enzymes possess high FNR activity but with measurable differences in affinity for different types of Fds as compared to other more conventional FNRs.

## Introduction

Ferredoxin (Fd) is a low molecular weight iron-sulfur protein that acts as an electron mediator in a variety of metabolic processes such as photosynthesis, nitrogen fixation, sulfate assimilation, etc. On the other hand, the reduction of Fd is catalyzed by a limited number of processes, such as electron donation from the type I photosynthetic reaction center, some type of hydrogenase, pyruvate-Fd oxidoreductase, and Fd-$NAD(P)^+$ oxidoreductase ([EC 1.18.1.2] and [EC 1.18.1.3], FNR). In oxygenic photosynthetic organisms, FNR plays a pivotal role in the reduction of $NADP^+$ to NADPH by using reduced Fd supplied by the photosystem I photochemical reaction [1], and the NADPH is subsequently used for carbon assimilation by the Calvin-Benson cycle, etc. In many heterotrophs, FNRs or its isoforms, adrenodoxin reductase (AdR) in vertebrates [2, 3] and putidaredoxin reductase (PdR) in some bacteria such as *Pseudomonas* species [4], catalyze the reaction in the direction of NAD(P)H oxidation and reduction of iron-sulfur proteins, which are subsequently used as electron donors to cytochrome P450.

FNR catalyzes electron transfer between the two-electron carrier nucleotide, NAD(P)H, and one-electron carrier iron-sulfur proteins such as Fd, adrenodoxin (Ad) and putidaredoxin (Pd), and also a low molecular weight flavoprotein called flavodoxin (Fld) which functions as a one-electron carrier under physiological conditions. FNRs are distributed over a wide variety of organisms and can be classified into four groups based on molecular phylogenetic analysis [5-9]. The first group of FNRs found in plants and cyanobacteria (referred to as the plastid-type FNR in this communication) participate in the redox reaction between [2Fe-2S]-type Fd (or Fld) and $NADP^+$/NADPH, which is used for carbon assimilation, glutamate synthesis, etc. [10]. The second group of FNRs are found in proteobacteria such as *Escherichia coli* [11] *Azotobacter vinelandii* [12] and *Rhodobacter capsulatus* [13, 14] (referred to as the proteobacteria-type

FNR), and the genes are notably induced under oxidative stress in these bacteria. The Fd reduction activity of proteobacterial FNRs is generally low (typically 0.15 ~ 3 $s^{-1}$) [14, 15]. FNR of the above two groups occurs and functions as a monomer.

AdR [2, 3], PdR [4] and some FNRs from bacteria such as *Mycobacterium tuberculosis*, *Rhodopseudomonas palustris* RPA3782 [16-18] make up the third FNR group (referred to as the mitochondria-type FNR), which perform the reduction of cytochrome P450 via the iron sulfur proteins (Ad and Pd) and generally occur as monomers, except for BphA4 from *Pseudomonas* sp. strain KKS102 which occurs as a dimer [19]. Because of the higher redox potentials of Ad and Pd, the reaction is directed toward oxidation of NAD(P)H and the reaction is practically irreversible. The amino acid sequences and three-dimensional structure of the third group FNRs are distinct from those of the FNRs of the former two groups and related to those of glutathione reductases that generally occur as homo-dimers [5-7, 20].

More recently, the fourth type of FNRs have been discovered in the green sulfur bacterium *Chlorobaculum tepidum* (syn. *Chlorobium tepidum*) [8] and the low-GC content Gram-positive bacterium *Bacillus subtilis* [9]. These FNRs occur as homo-dimers, and show high amino acid sequence identity with thioredoxin reductases, but lack the two-cysteine motif essential for the catalysis of the latter enzymes. From database searches for genes encoding proteins with high amino acid sequence identity to these types of FNR, homologous genes are found in many Gram-positive bacteria (Firmicutes), green sulfur bacteria, some $\alpha$-proteobacteria and archaea [9]. These FNRs will be referred to as the Firmicutes and green sulfur bacteria-type FNR. Some bacteria such as *Rhodopseudomonas palustris* CGA009 have three FNRs, the plastid-type (RPA1578), the mitochondria-type (RPA3782) and the fourth type (RPA3954).

Although the four FNR group enzymes differ from each other in the overall amino acid sequence, they possess a common two-nucleotide-binding-domain architecture, one for FAD or

FMN and the other for $NAD(P)^+$/ NAD(P)H in the N-terminus and C-terminus, respectively. This architecture is typical of the $NAD(P)^+$/NAD(P)H-linked flavoenzyme family including disulfide reductases such as glutathione reductase and thioredoxin reductase [5-7, 20]. Because FNRs have multiple phylogenetic origins, comparative studies of different FNR group enzymes with respect to the mechanisms regulating substrate binding and catalytic properties are necessary for a deeper understanding of the structure-function relationships of FNR. With monomeric FNRs of the plastid-type and the mitochondria-type, substrate binding and reaction mechanisms have been extensively studied [for reviews, see 6, 7, 10, 21]. However, few such studies have been reported on the proteobacteria-type [14, 15] and no such studies have been reported on the Firmicutes and green sulfur bacteria-type FNRs.

In the present communication, we have chosen two FNRs from the fourth group, namely, *B. subtilis* FNR (YumC) which has previously been purified and biochemically characterized [9] and *Rhodopseudomonas palustris* FNR (RPA3954) which has not yet been purified. We studied their reactivity with $NAD(P)^+$/NAD(P)H and Fds by steady-state kinetic analysis and by measuring difference spectra induced by addition of these substrates. In contrast with the plastid-type FNRs which react with both [2Fe-2S] and [4Fe-4S] type Fds at comparable rates [22], the reduction rates of YumC and *R. palustris* FNR for [2Fe-2S] type Fds from spinach and *R. palustris* (RPA3956) were much lower than those for *B. subtilis* [4Fe-4S] Fd. From steady state reaction data analyses reported here, a redox reaction mechanism involving ternary complex formation is suggested for the YumC-*B. subtilis* Fd system.

## 2. Materials and methods

### *2.1. Preparation of FNRs and Fds*

The following gene products were overexpressed in *E. coli,* and purified as described in Supplementary data section: FNR gene *yumC* of *B. subtilis* subsp. *subtilis str. 168* (NCBI GeneID 936577, [23]), FNR gene of *R. palustris* CGA009 (RPA3954, NCBI GeneID 2690535, [24]), [4Fe-4S] type Fd gene of *B. subtilis* (*ypbA*, Pub-Med ID 938968 [23]), [2Fe-2S] type Fd gene of *R. palustris* CGA009 (RPA3956, NCBI GeneID 2689967 [24]). Spinach [2Fe-2S] type Fd was purified according to the procedure described in [25].

### *2.2. Enzymatic activity assays*

In the following assays, blanks consisted of all assay reagents except FNRs.

NAD(P)H diaphorase activity was assayed with ferricyanide ($\varepsilon_{420}$ = 1.02 $mM^{-1}$ $cm^{-1}$, or $\varepsilon_{440}$ = 0.59 $mM^{-1}$ $cm^{-1}$) as the electron acceptor in 100 mM potassium phosphate buffer (pH 7.0). The reaction mixture (1 ml) contained 3 mM potassium ferricyanide for YumC or 1 mM for *R. palustris* FNR (RPA3954), 5 mM glucose 6-phosphate (G6P, G7250, Sigma Chemical Co.), 5 U of glucose-6-phosphate dehydrogenase (G6PDH, *Leuconostoc mesenteroides*, G8404, Sigma) and 5–10 nM FNRs together with NAD(P)H as indicated in the figure legends and table.

NAD(P)H oxidase assay was performed according to the procedure described in [9].

NAD(P)H-cytochrome *c* reductase activity was assayed under aerobic conditions by monitoring the increase in the absorbance at 550 nm with horse heart cytochrome *c* ($\Delta\varepsilon_{550}$ = 21 $mM^{-1}cm^{-1}$, Sigma). The reaction mixture (1 ml) contained 0.1 mM cytochrome *c* from horse heart, 5 mM G6P, 5 U G6PDH, 20 μM NADPH and 10 nM FNRs in 100 mM potassium phosphate buffer (pH 7.0).

For the Fd-dependent cytochrome *c* reduction activity under aerobic conditions, the assay

mixtures (0.5 or 1 ml) contained 0.1 mM cytochrome *c* from horse heart, 5 mM G6P, 5 U/ml G6PDH, and 1–10 nM FNRs together with NAD(P)H and Fds in 100 mM potassium phosphate buffer (pH 7.0). Enzymatic activities are expressed by subtraction the values of the respective assay blank containing all the assay reagents except FNRs.

Turnover rates are expressed as the number of NAD(P)H molecules oxidized by one molecule of native-form FNRs per second. Each data point in Figure 4-6 is the average of 3 to 4 independent measurements.

*2.3. Spectral measurements*

The UV-visible (UV-Vis) absorption spectra were measured with a double beam spectrophotometer (V-560, JASCO, Tokyo, Japan). The spectra of the reduced YumC (18 μM in 100 mM potassium phosphate buffer (pH 7.0)) and *R. palustris* FNR (RPA3954) (14 μM in 100 mM potassium phosphate buffer (pH 7.0)) were obtained after a few minutes of incubation in the presence of a 10-fold excess amount of NADPH, or after 30 min of incubation at 4˚C with an excess amount of dithionite under anaerobic conditions. For $K_d$ determination, each 1–10 μl of either $NADP^+$ (0.01 – 100 mM) or [4Fe-4S] type of Fd of *B. subtilis* (1.22 mM) stock solutions were added to the cuvettes containing YumC or *R. palustris* FNR as indicated in 2 ml of 100 mM potassium phosphate buffer (pH 7.0). Spectra were measured after few minutes' incubation at room temperature. The experimentally obtained spectra were corrected for the volume changes, and difference spectra were calculated by subtracting the control spectrum recorded prior to addition of substrates from the corrected ones. For determinations of the relationship between the temperature and the reaction rate, a thermoelectrically temperature controlled cell holder was used.

*2.4. Data analysis*

Non-linear regression data analysis was performed with Igor 5.0.2 software (WaveMetrics). The $K_d$ values for $NADP^+$ and Fd were determined by fitting to the equation described in Batie and Kamin [26]. The steady-state reaction data in Fig. 6 were fitted to Eq. 1 for a rapid equilibrium bi-reactant system.

$$\frac{V_{max}\,[NADPH][Fd]}{\kappa_s K_m^{N} + K_m^{F}[NADPH] + K_m^{N}[Fd] + [NADPH][Fd]}$$

In Eq. 1, $v$ is the initial steady-state reaction velocity, $V_{max}$ is the maximum reaction velocity, $K_m^{F}$ and $K_m^{N}$ are the concentrations that give a half velocity of $V_{max}$ for Fd and NADPH (the Michaelis-Menten constants), respectively, and $K_s$ is the inhibition constant. Except for the above cases, kinetic constants were obtained by fitting to the Michalis-Menten equation.

The values of the activation energy change $\Delta H^{\ddagger}$ were obtained from the slopes of the plot in Fig. 5 based on the equation $\log(k/T) = \log(R/Nh)+\Delta S^{\ddagger}/2.303R-\Delta H^{\ddagger}/2.303RT$, where $T$ is the absolute temperature, $R$ is the gas constant, $N$ is Avogadro's number, and $h$ is Planck's constant.

The following concentrations of the substrates and enzymes were determined based on the absorption coefficients for YumC ($\varepsilon_{457}$ = 12.3 $mM^{-1}$ $cm^{-1}$, [8]), *B. subtilis* Fd ($\varepsilon_{390}$ = 16.0 $mM^{-1}$ $cm^{-1}$ [28]), [2Fe-2S] type of Fd of *R. palustris* (RPA3956, $\varepsilon_{410}$ = 9.56 $mM^{-1}$ $cm^{-1}$ [28]), spinach Fd ($\varepsilon_{420}$ = 9.68 $mM^{-1}$ $cm^{-1}$) and NAD(P)H ($\varepsilon_{340}$ = 6.2 $mM^{-1}$ $cm^{-1}$). The absorption coefficient of *R. palustris* FNR (RPA3954) was determined according to the method described in [29]. Briefly, the enzyme was treated with trichloroacetic acid (5%, w/v), and the flavin concentration in the neutralized supernatant (pH 7.0) was determined from $\varepsilon_{450}$ = 11.3 $mM^{-1}$ $cm^{-1}$.

DNA sequence data of *B. subtilis* FNR gene *yumC*, *R.palustris* FNR gene RPA3954, *R. palustris* [2Fe-2S] type Fd gene RPA3956 and *B. subtilis* [4Fe-4S] type Fd gene *fer* were

obtained from the GenomeNet Server (http://www.genome.ad.jp, Kyoto University). Sequence alignment was performed using CLUSTAL W [30] on the GenomeNet server.

## 3. Results

### *3.1. Expression of FNRs and Fds*

The recombinant proteins described in Materials and methods section were successfully expressed and subsequently purified to apparent homogeneity (see, Supplementary data section).

We found from sequencing the *B. subtilis yumC* in the pETBlue-1 plasmid construct that it differed from the one registered in the complete genomic DNA sequence of *B. subtilis* (Pub-Med GeneID 936577, [23], Fig. 1A). Our *yumC* sequence has a single nucleotide insertion of adenosine (a) between positions 312 and 313, and a single nucleotide deletion of guanosine (g) in position 348 as compared to the registered sequence. Accordingly, the deduced 12-amino acid sequences in this region differed considerably from each other (Fig. 1B). In this paragraph only, our *yumC* sequence and the deduced protein will be referred to as *yumC*(K) and YumC(K), respectively, in order to distinguish them from the registered one (*yumC*) and its product. FNR genes have been reported for four other *Bacillus* strains, and the consensus amino acid sequence of the four deduced proteins of other *Bacillus* species agrees with YumC(K), but not with YumC (Fig. 1B). In the previous report [9], we purified FNR from wild-type *B. subtilis* cells, sequenced its N-terminus, and found that the first 17-amino acid sequence completely agreed with the one deduced from the registered nucleotide sequence of *yumC*, which was also in agreement with the *yumC*(K) sequence. No significant difference was found in UV-Vis absorption spectra between YumC(K) (Fig. 2A) and YumC prepared from wild-type *B. subtilis* cells [9]. These results indicate the need for a reexamination of the *yumC* sequence in the future. Throughout this study, the recombinant YumC(K) (hereafter YumC) was used.

The DNA sequences of *R. palustris* FNR (RPA3954) (hereafter *R. palustris* FNR), *B. subtilis* [4Fe-4S] type Fd and *R. palustris* [2Fe-2S] type Fd (RPA3956) in the plasmids used in

this communication completely agreed with the registered sequences ([23, 24]), and the properties of the expressed protein essentially agreed with those reported for the preparations purified from the wild-type cells; *B. subtilis* [4Fe-4S] type Fd: UV-Vis and EPR spectra [27], and *R. palustris* [2Fe-2S] type Fd: UV-Vis and EPR spectra (Figs. S3, S4, [28]). Because *B. subtilis* Fd was unstable under conditions of low ionic strength, we used buffers of 50 mM Tris-HCl (pH 8.0) containing 100 mM NaCl for dialysis, and the purified Fd was stored in 50 mM Tris-HCl buffer (pH 8.0) containing 300 mM NaCl.

The molecular masses of recombinant YumC and *R. palustris* FNR polypeptides were both deduced to be about 38 kDa from the DNA sequences, and found to be about 40 and 38 kDa on SDS-PAGE analysis (Fig. S1, Supplementary data), respectively. The apparent molecular masses of native YumC and *R. palustris* FNR were found to be about 98 and about 67 kDa, respectively, by gel permeation chromatography (Fig. S2). These results indicate that both FNRs exist as homo-dimeric proteins under the experimental conditions used in this study.

*3.2. Difference absorption spectra induced by oxidation-reduction and substrate addition*

UV-Vis absorption spectrum of air-oxidized YumC is a typical of flavoproteins, with peaks at 457 and 383 nm and a shoulder at 490 nm (Fig. 2A, continuous line). *R. palustris* FNR has peaks at 464 and 377 nm and a shoulder at 490 nm (Fig. 2B, continuous line), and its absorption coefficient per subunit was calculated to be 10.8 $mM^{-1}$ $cm^{-1}$ at 464 nm from determination of FAD in the extract of the denatured protein.

In the presence of a 10-fold excess amount of NADPH under anaerobic conditions, the peak in about 400-500 nm region became smaller and broad absorption bands appeared in about the 450–750 nm region in both of the FNRs (Fig. 2A, B, dotted lines). Because these spectra were obtained in the absence of one-electron carriers, the spectral changes in the latter region

are ascribed to formation of charge-transfer species: FAD-NADPH and $FADH_2$-$NADP^+$ [31, 32]. When FNRs were fully reduced in the presence of excess amounts of dithionite in the absence of $NADP^+$, the peak in about the 400-500 nm region was much lower than that of the oxidized form and the broad absorption band in about the 550–750 nm region was not found (Fig. 2A, B, broken lines).

Interactions of FNRs with $NADP^+$ and *B. subtilis* Fd were studied by UV-Vis difference optical absorption measurements (Fig. 3). When 1 mM $NADP^+$ was mixed with YumC, the difference spectrum gave troughs at 449 and 481 nm, and peaks at 469 and 505 nm (Fig. 3A, (**a**)). With *R. palustris* FNR, troughs were found at 458 and 487 nm, and peaks at 473 and 507 nm (Fig. 3B (**a**)). When YumC was mixed with *B. subtilis* Fd, difference spectra exhibited troughs at 400, 470 and 500 nm with YumC (Fig. 3A(**b**)). With *R. palustris* FNR, in addition to the peaks 394, 475, 510, a very low trough at 700 nm appeared (Fig. 3B (**b**)). When both *B. subtilis* Fd and $NADP^+$ were added to YumC, the difference spectrum (Fig. 3A (**c**)) differed from the sum of the difference spectrum induced by each of the two ((**d**) = (**a**) + (**b**)). Compared with spectrum (**d**), the magnitude of spectrum (**c**) in about the 400-490 nm region was greatly decreased, indicating that the affinity of FNR for Fd would be decreased by the addition of $NADP^+$.

The plots of the magnitude of the spectral changes $\Delta\varepsilon_{507} - \Delta\varepsilon_{484}$ for Yum C and $\Delta\varepsilon_{506} - \Delta\varepsilon_{481}$ for *R. palustris* FNR against the concentrations of $NADP^+$ yield saturation curves (Fig. 3C), indicating that spectral changes in these regions are largely due to binding of $NADP^+$. Similarly, the plots of $\Delta\varepsilon_{382} - \Delta\varepsilon_{404}$ for Yum C and $\Delta\varepsilon_{381} - \Delta\varepsilon_{398}$ for *R. palustris* FNR against the concentrations of *B. subtilis* Fd (Fig. 3D) yield saturation curves, indicating that spectral changes in these regions are largely due to binding of *B. subtilis* Fd. The dissociation constants ($K_d$) of YumC and *R. palustris* FNR for $NADP^+$ were estimated to be 14 ± 3 μM and 41 ± 4 μM,

respectively (Fig. 3C, Table 1). The dissociation constants ($K_d$) of YumC and *R. palustris* FNR for *B. subtilis* Fd was estimated to be 1.7 ± 0.3 μM and 32 ± 5 μM, respectively (Fig. 3D, Table 1).

*3.3. Reactivity with NAD(P)H, ferricyanide and Fd*

The effects of *B. subtilis* Fd on cytochrome *c* reduction by both of the FNRs were studied under aerobic conditions. As for the NADPH concentration dependency, the reaction rate with *R. palustris* FNR in the presence of 5 μM *B. subtilis* Fd initially increased with an increase in NADPH concentration, but decreased at concentrations of > 100 μM. The inhibitory effects of high concentrations of NADPH were lower than on YumC (Fig. 4). In the presence of [2Fe-2S] type Fds from spinach and *R. palustris* (RPA3956, [24]) (Table 1), both FNRs supported Fd reduction with a lower rate than [4Fe-4S] type Fd from *B. subtilis*.

The $K_m$ values for ferricyanide of YumC were found to be 250 ± 30 μM at an NADPH concentration of 0.5 mM. This concentration of NADPH also gave almost the highest activity, because NADPH decreased the apparent affinity for ferricyanide, and vice versa (data not shown). At a ferricyanide concentration of 2.9 mM, the $K_m$ value for NADPH and the $k_{cat}$ value were determined to be 10.9 ± 0.2 μM and 900 ± 40 $s^{-1}$, respectively (Table 1). With *R. palustris* FNR, the $K_m$ value for ferricyanide was estimated to be 29 ± 5 μM at an 1 mM NADPH. At 1 mM ferricyanide, the $K_m$ values for NADPH and $k_{cat}$ were estimated to be 45 ± 3 μM and 346 ± 7 $s^{-1}$, respectively (Table 1). With NADH, *R. palustris* FNR exhibited a reduction rate of 11 ± 1 $s^{-1}$ at 1 mM NADH and 1 mM ferricyanide.

Some flavoenzymes oxidize NAD(P)H, utilizing molecular oxygen as an electron acceptor (referred to as NAD(P)H oxidase activities in Table 1). *R. palustris* FNR shows low NAD(P)H oxidase activity (Table 1), in contrast to *C. tepidum* FNR that has much higher oxidase activity

[8]. Many monomeric proteobacteria-type FNRs have high cytochrome *c* reduction activity by NADPH in the absence of Fd [15], however, both YumC and *R. palustris* FNR have low cytochrome *c* reduction activities (Table 1).

From measurements of the temperature dependence of the reaction rates, the$\Delta H^{\ddagger}$ values of YumC for diaphorase activity with ferricyanide and Fd-dependent cytochrome *c* reduction activity at pH 7.0 under aerobic conditions, were estimated to be 21 ± 1 kJ $mol^{-1}$ and 40 ± 3 kJ $mol^{-1}$, respectively. With *R. palustris* FNR NADPH diaphorase activity with ferricyanide, the value of $\Delta H^{\ddagger}$ was estimated to be 21 ± 4 kJ $mol^{-1}$, which is almost the same as that of YumC. (Fig. 5)

*3.4. Steady-state kinetic analysis of B. subtilis FNR*

The steady-state reaction rates of YumC for NADPH- and Fd-dependent cytochrome *c* reduction assayed at various concentrations of NADPH and *B. subtilis* Fd under aerobic conditions are presented as a double-reciprocal plot in Fig. 6. The rate increased with increasing NADPH concentration, reaching a maximum at around 10 μM NADPH and then declined at each fixed Fd concentration (Fig. 4, 6). By nonlinear regression analysis with the data points at the NADPH concentration of 0–2 μM, maximum rate and Michaelis-Menten constants in Eq. 1 were estimated. The values were; $V_{max}$ value of 99 ± 6 $s^{-1}$, $K_m^N$ value of 0.19 ± 0.04 μM (for NADPH), $K_m^F$ value of 2.7 ± 0.3 μM (for Fd) and $K_s$ value of 1.2 ± 0.6 μM (Table 1).

## 4. Discussion

In spite of their different phylogenetic origins, YumC and *R. palustris* FNR share several common characteristics with other types of FNRs: an increase in absorbance in about the 550-750 nm region in the presence of NADPH (Fig. 2) [16, 31, 32] which can be attributed to formation of charge transfer species: [NADPH-FAD] and [$NADP^+$-$FADH_2$] [31, 32].

YumC and *R. palustris* FNR display reaction kinetics similar to each other, as noted in this communication, but there are some marked differences. Although the obtained difference spectra for $NADP^+$ binding of YumC and *R. palustris* FNR were similar, the reduction rate of *R. palustris* FNR by NADPH was lower, and $K_d$ for $NADP^+$ and $K_m$ for NADPH values were higher than those of YumC (Fig. 3C, Table 1). Within the thioredoxin reductase superfamily, it has been reported that the $Gly^{152}$-Gly-Gly-X-X-$Ala^{157}$ motif (numbering from the *E. coli* TR) is related to NAD(P)H specificity [33-37] and additionally, the $His^{175}$ and $Arg^{177}$ residues have been shown to interact with the 2'-phosphate group of $NADP^+$ and the $Arg^{181}$ residue with the pyrophosphate and the adenine ribose of $NADP^+$ in NADPH-thioredoxin reductases of *Arabidopsis thaliana* [33] and *E. coli* [34], whereas these residues are substituted in NADH dependent oxidoreductases [35-37]. Among members of the Firmicutes and green sulfur bacteria-type FNR, *C. tepidum* FNR reacts with both $NAD^+$/NADH and $NADP^+$/NADPH without significant discrimination [8], whereas YumC and *R. palustris* FNR strongly discriminate against $NAD^+$/NADH (Table 1). Within *C. tepidum* FNR, *B. subtilis* YumC, *R. palustris* FNRs and also *Sulfolobus* NADH oxidase, the $Gly^{152}$-$Ala^{157}$ and $His^{175}$ residues in TR are conserved in their corresponding sequences. However, in the deduced sequence of *C. tepidum* FNR, the residues corresponding to the $Arg^{177}$ and $Arg^{181}$ residues in TR are substituted to the $Gly^{195}$ and $Gln^{199}$ residues. On the other hand, $Arg^{177}$ and $Arg^{181}$ in TR are completely conserved in *B. subtilis* YumC, *R. palustris* FNR and *Sulfolobus* NADH oxidase, and all show

much higher reactivity to NADPH than to NADH [38]. Thus the residues important for nucleotide binding in the disulfide reductase family seem to be conserved in the members of the fourth group of FNRs. The residues $Arg^{177}$ and $Arg^{181}$ seem to be important for discriminating between NADPH and NADH by interacting with the negative charge on the phosphoryl anion residue bound to the 2' position of NADPH. From the difference in $K_d$ (14 μM for YumC vs. 41 μM for *R. palustris* FNR) and $K_m$ (10.9 μM for YumC vs. 45 μM for *R. palustris* FNR) values for $NADP^+$ and NADPH between YumC and *R. palustris* FNR suggested there is another factor(s) that greatly affects the affinity. With pea chloroplast and *Anabaena* PCC7119 FNRs, $Tyr^{308}$ in the pea FNR and $Tyr^{303}$ in the *Anabaena* FNR near the C-terminus were shown to be important for exerting a high discrimination between NADPH and NADH in favour of the former. [39, 40].

When *R. palustris* FNR was mixed with *B. subtilis* Fd, a very small negative peak appeared around 700 nm. Such a spectral change was not observed with YumC, and the reason for these different behaviours between the two remains to be investigated.

The NADPH diaphorase activity of YumC with ferricyanide as the electron acceptor was ~ 900 $s^{-1}$, which is similar to those of the plastid-type FNRs (~ 550 $s^{-1}$) [21]). The dissociation constant value for $NADP^+$ is also similar to those of the plastid-type FNRs (14 μM for YumC versus 6 and 15 μM for spinach and *Anabaena* FNR, respectively [21]). However, differences between YumC and other types of FNRs were observed for Fd dependent cytochrome *c* reduction activity (~ 45 $s^{-1}$, Fig. 4, and Table 1), which was lower than those of the plastid-type FNR-Fd systems (~ 250 $s^{-1}$ [21]) and mitochondoria-type PdR-PdR systems (550 $s^{-1}$ [41]), and higher than those of proteobacteria-type FNR-Fd systems (typically 0.15 ~ 3 $s^{-1}$ [14, 15]) and mitochondoria-type AdR-Ad systems (typically 4.5 $s^{-1}$ [42]). YumC and *R. palustris* FNRs showed remarkably low reactivities toward [2Fe-2S] type Fd, which were more than 60-fold

lower than those for [4Fe-4S] type Fd reduction (Table 1). This is in contrast with the other types of FNRs whose physiological electron donor/acceptors are considered to be [2Fe-2S] type Fds, and they react with [4Fe-4S] type Fds as well [22]. Such a low rate of reduction toward [2Fe-2S] type Fd may be one of the reasons why the fourth type of FNR is not shared among eukaryotes and $\gamma$-proteobacteria that utilize [2Fe-2S] type Fds.

*R. palustris* is known as a metabolically diverse organism and has three putative FNR genes in its genome [24], each belonging to the different types, namely plastid-type (*fpr*, RPA1578), mitochondoria-type (RPA3782) and Firmicutes and green sulfur bacteria-type (RPA3954) defined in this paper. The presence of multiple FNR isoforms as in *R. palustris* has not been found in other genomes reported thus far except for several $\alpha$-proteobacteria. Although the *fpr* (RPA1578) homologue from *Rhodobacter capsulatus* was expressed in *E. coli* and the details of its reaction behavior were characterized, its physiological electron acceptor protein was not identified [14]. In this work, we demonstrated that *R. palustris* FNR (RPA3954) exhibits high Fd reduction activity and low NAD(P)H oxidase activities, which suggest that RPA3954 functions as a component for the Fd reduction pathway in the bacterium, although the physiological electron donor/acceptor and related metabolism remain unknown. Further investigations of the Fds, and Fd-related enzymes will be needed to understand the metabolic diversity of this bacterium and the diversity of the Fd-FNR systems.

**Acknowledgement**

We thank Dr. Hidehiro Sakurai for stimulating discussions and suggestions. This work was partly supported by the Life Science foundation of Japan to D. S.

**References**

[1]M. Shin, K. Tagawa, D.I. Arnon. Crystallization of ferredoxin-TPN reductase and its role in the photosynthetic apparatus of chloroplasts. Biochem Z. 338(1963)84-96.

[2]T. Omura, E. Sanders, R.W. Estabrook, D.Y. Cooper, O. Rosenthal. Isolation from adrenal cortex of a nonheme iron protein and a flavoprotein functional as a reduced triphosphopyridine nucleotide-cytochrome P-450 reductase. Arch. Biochem. Biophys. 117 (1966) 660-673.

[3]J.W. Chu, T. Kimura, Studies on adrenal steroid hydroxylases. Molecular and catalytic properties of adrenodoxin reductase (a flavoprotein), J. Biol. Chem. 248 (1973) 2089-2094.

[4]M. Katagiri, B.N. Ganguli, I.C. Gunsalus, A soluble cytochrome P-450 functional in methylene hydroxylation, J. Biol. Chem. 243 (1968) 3543-3546.

[5]I. Hanukoglu, T. Gutfinger, M. Haniu, J.E. Shively, Isolation of a cDNA for adrenodoxin reductase (ferredoxin-$NADP^+$ reductase). Implications for mitochondrial cytochrome P-450 systems, Eur. J. Biochem. 169 (1987) 449-455.

[6]E.A. Ceccarelli, A.K. Arakaki, N. Cortez, N. Carrillo, Functional plasticity and catalytic efficiency in plant and bacterial ferredoxin-NADP(H) reductases, Biochim. Biophys. Acta. 1698 (2004)155-165.

[7]A. Aliverti, V. Pandini, A. Pennati, M. de Rosa, G. Zanetti. Structural and functional diversity of ferredoxin-NADP(+) reductases. Arch Biochem Biophys. Arch Biochem Biophys. 474 (2008) 283-291.

[8]D. Seo, H. Sakurai, Purification and characterization of ferredoxin-$NADP^+$ reductase from the green sulfur bacterium *Chlorobium tepidum*, Biochim. Biophys. Acta 1597 (2002)123-132.

[9]D. Seo, K. Kamino, K. Inoue, H. Sakurai, Purification and characterization of ferredoxin-$NADP^+$ reductase encoded by *Bacillus subtilis yumC*, Arch. Microbiol. 182 (2004) 80-89.

[10]D.B. Knaff, M. Hirasawa, Ferredoxin-dependent chloroplast enzymes, Biochim. Biophys. Acta 1056 (1991) 93-125.

[11]V. Bianchi, P. Reichard, R. Eliasson, E. Pontis, M. Krook, H. Jornvall, E. Haggard- Ljungquist,

*Escherichia coli* ferredoxin $NADP^+$ reductase: Activation of *E. coli* anaerobic ribonucleotide reduction, cloning of the gene (*fpr*), and overexpression of the protein, J. Bacteriol. 175 (1993) 1590-1595.

[12]J.M. Isas, I.S.M. Yannone, B.K. Burgess, *Azotobacter vinelandii* NADPH:ferredoxin reductase cloning, sequencing, and overexpression, J. Biol. Chem. 270 (1995) 21258-21263.

[13]C. Bittel, L.C. Tabares, M. Armesto, N. Carrillo, N. Cortez, The oxidant-responsive diaphorase of *Rhodobacter capsulatus* is a ferredoxin (flavodoxin)-NADP(H) reductase, FEBS Letters 553 (2003) 408-412.

[14]I. Nogués, I. Pérez-Dorado, S. Frago, C. Bittel, SG. Mayhew, C. Gómez-Moreno, JA. Hermoso, M. Medina, N. Cortez, N. Carrillo, The ferredoxin-NADP(H) reductase from *Rhodobacter capsulatus*: molecular structure and catalytic mechanism., Biochemistry 44 (2005) 11730-11740.

[15]J.T. Wan JT, J.T. Jarrett, Electron acceptor specificity of ferredoxin (flavodoxin):NADP oxidoreductase from *Escherichia coli*, Arch. Biochem. Biophys. 406 (2002) 116-126.

[16]F. Fischer, D. Raimondi, A. Aliverti, G. Zanetti, *Mycobacterium tuberculosis* FprA, a novel bacterial NADPH-ferredoxin reductase, Eur. J. Biochem. 269 (2002) 3005-3013.

[17]K.J. McLean, N.S. Scrutton, A.W. Munro, Kinetic, spectroscopic and thermodynamic characterization of the *Mycobacterium tuberculosis* adrenodoxin reductase homologue FprA, Biochem. J. 372 (2003) 317-327.

[18]Y. Peng, F. Xu, SG. Bell, LL. Wong, Z. Rao, Crystallization and preliminary X-ray diffraction studies of a ferredoxin reductase from Rhodopseudomonas palustris CGA009, Acta Crystallogr. Sect. F Struct. Biol. Cryst. Commun. 63 (2007) 422-5.

[19]T. Senda, T. Yamada, N. Sakurai, M. Kubota, T. Nishizaki, E. Masai, M. Fukuda, Y. Mitsui, Crystal structure of NADH-dependent ferredoxin reductase component in biphenyl dioxygenase, J. Mol. Biol. 304 (2000) 397-410.

[20]G.A. Ziegler, C. Vonrhein, I. Hanukoglu, G.E. Schulz, The structure of adrenodoxin reductase of mitochondrial P450 systems: electron transfer for steroid biosynthesis, J. Mol. Biol. 289 (1999) 981-990.

[21]N. Carrillo, E.A. Ceccarelli, Open questions in ferredoxin-NADP$^+$ reductase catalytic mechanism, Eur. J. Biochem. 270 (2003) 1900-1915.

[22]D. Seo, A. Tomioka, N. Kusumoto, M. Kamo, I. Enami, H. Sakurai, Purification of ferredoxins and their reaction with purified reaction center complex from the green sulfur bacterium *Chlorobium tepidum*, Biochim Biophys Acta. 1503 (2001) 377-84.

[23]F. Kunst, N. Ogasawara, I. Moszer, A.M. Albertini, G. Alloni, V. Azevedo, M.G. Bertero, P. Bessieres, A. Bolotin, S. Borchert, R. Borriss, L. Boursier, A. Brans, M. Braun, S.C. Brignell, S. Bron, S. Brouillet, C.V. Bruschi, B. Caldwell, V. Capuano, N.M. Carter, S.K. Choi, J.J. Codani, I.F. Connerton, A. Danchin, et al, The complete genome sequence of the gram-positive bacterium *Bacillus subtilis*, Nature 390 (1997) 249-256.

[24]FW. Larimer, P. Chain, L. Hauser, J. Lamerdin, S. Malfatti, L. Do, ML. Land, DA. Pelletier, JT. Beatty, AS. Lang, FR. Tabita, JL. Gibson, TE. Hanson, C. Bobst, JL. Torres, C. Peres, FH. Harrison, J. Gibson, CS. Harwood, Complete genome sequence of the metabolically versatile photosynthetic bacterium *Rhodopseudomonas palustris*. Nature Biotechnol. 22 (2004) 55-61.

[25]M. Shin, A guide for biochemical approach to ferredoxin-NADP reductase system (in Japanese), Tanpakushitsu Kakusan Koso 21 (1976) 226-232.

[26]C.J. Batie, H. Kamin, Ferredoxin:NADP$^+$ oxidoreductase. Equilibria in binary and ternary complexes with NADP$^+$ and ferredoxin, J. Biol. Chem. 259 (1984) 8832-8839.

[27]A.J. Green, A.W. Munro, M.R. Cheesman, G.A. Reid, C. Von Wachenfeldt, S.K. Chapman, Expression, purification and characterisation of a *Bacillus subtilis* ferredoxin: A potential electron transfer donor to cytochrome P450 BioI, J. Inor. Biochem. 93 (2003) 92-99.

[28]I. Naud, M. Vinçon, J. Garin, J. Gaillard, E. Forest, Y. Jouanneau, Purification of a sixth ferredoxin from Rhodobacter capsulatus. Primary structure and biochemical properties, Eur. J. Biochem. 222 (1994) 933-939.

[29]K. Ohnishi, Y. Niimura, K. Yokoyama, M. Hidaka, H. Masaki, T. Uchimura, H. Suzuki, T. Uozumi, M. Kozaki, K. Komagata, T. Nishino, Purification and analysis of a flavoprotein functional as NADH oxidase from *Amphibacillus xylanus* overexpressed in *Escherichia coli*, J. Biol. Chem.

269 (1994) 31418-31423.

[30]J.D. Thompson, D.G. Higgins, T.J. Gibson, CLUSTAL W: improving the sensitivity of progressive multiple sequence alignment through sequence weighting, position-specific gap penalties and weight matrix choice, Nucleic Acids Res. 22 (1994) 4673-4678.

[31]J. Tejero, JR. Peregrina, M. Martínez-Júlvez, A. Gutiérrez, C. Gómez-Moreno, NS. Scrutton, M. Medina, Catalytic mechanism of hydride transfer between NADP+/H and ferredoxin-NADP+ reductase from Anabaena PCC 7119, Arch. Biochem. Biophys. 459 (2007) 79-90.

[32]V. Massey, R.G. Matthews, G.P. Foust, L.G. Howell, C.H. Williams Jr., G. Zanetti, S. Ronchi, A new intermediate in TPNH-linked flavoproteins, in H. Sund (Eds.), Pyridine Nucleotide-dependent Dhydrogenases, Springer-Verlag, Berlin, 1970, pp. 393-411.

[33]S. Dai, M. Saarinen, S. Ramaswamy, Y. Meyer, J.P. Jacquot, H. Eklund, Crystal structure of *Arabidopsis thaliana* NADPH dependent thioredoxin reductase at 2.5 Å resolution, J. Mol. Biol. 264 (1996) 1044-1057.

[34]G. Waksman, T.S. Krishna, C.H. Williams Jr., J. Kuriyan, Crystal structure of *Escherichia coli* thioredoxin reductase refined at 2 Å resolution. Implications for a large conformational change during catalysis, J. Mol. Biol. 236 (1994) 800-816.

[35]C.M. Reynolds, J. Meyer, L.B. Poole, An NADH-dependent bacterial thioredoxin reductase-like protein in conjunction with a glutaredoxin homologue form a unique peroxiredoxin (AhpC) reducing system in *Clostridium pasteurianum*, Biochemistry 41 (2002) 1990-2001.

[36]N.S. Scrutton, A. Berry, R.N. Perham, Redesign of the coenzyme specificity of a dehydrogenase by protein engineering, Nature 343 (1990) 38-43.

[37]I. Hanukoglu, T. Gutfinger, cDNA sequence of adrenodoxin reductase. Identification of NADP-binding sites in oxidoreductases, Eur. J. Biochem. 180 (1989) 479-484.

[38]P. Arcari, L. Masullo, M. Masullo, F. Catanzano, V. Bocchini, A NAD(P)H oxidase isolated from the archaeon *Sulfolobus solfataricus* is not homologous with another NADH oxidase present in the same microorganism. Biochemical characterization of the enzyme and cloning of the encoding gene, J. Biol. Chem. 275 (2000) 895-900.

[39]L. Piubelli, A. Aliverti, A.K. Arakaki, N. Carrillo, E.A. Ceccarelli, P. Andrew Karplus, G. Zanetti, Competition between C-terminal tyrosine and nicotinamide modulates pyridine nucleotide affinity and specificity in plant ferredoxin-$NADP^+$ reductase, J. Biol. Chem. 275 (2000) 10472-10476.

[40]J. Tejero, I. Pérez-Dorado, C. Maya, M. Martínez-Júlvez, J. Sanz-Aparicio, C. Gómez-Moreno, J.A. Hermoso, M. Medina, C-terminal tyrosine of ferredoxin-$NADP^+$ reductase in hydride transfer processes with $NAD(P)^+$/H, Biochemistry 44 (2005) 13477-13490.

[41]P.W. Roome, J.A. Peterson, The oxidation of reduced putidaredoxin reductase by oxidized putidaredoxin, Arch. Biochem. Biophys. 266 (1988) 41-50.

[42]J.D. Lambeth, H. Kamin, Adrenodoxin reductase. Properties of the complexes of reduced enzyme with $NADP^+$ and NADPH, J. Biol. Chem. 251 (1976) 4299-4306.

**Figure legends**

Fig. 1. (A) Alignment of the partial DNA sequence of the previously annotated *yumC* of *B. subtilis* subsp. *subtilis str. 168* (NCBI GeneID 936577) (1st line) and the one determined in this work (2nd line). The insertion (or the deletion in the counterpart) is shown in underlined bold face. (B) Partial amino acid sequence alignments of YumC and its homologues. The segments affected by the above insertion/deletion are underlined. The sequence data were obtained from the Genome Net server. Bsu_BG12391_yumC; yumC of *Bacillus subtilis* subsp. *subtilis str. 168*, Bld_BLi03393; *yumC* of *Bacillus licheniformis* DSM13, Bli_BL03143; *yumC* of *Bacillus licheniformis* ATCC 14580, bce_BC4926; thioredoxin reductase (TR) of *Bacillus cereus* ATCC 14579, baa_BA0033; pyridine nucleotide-disulphide oxidoreductase (POR) of *Bacillus anthracis* A2012. Consensus sequence among the latter four annotated *Bacillus* YumC homologues are represented between *Bacillus subtilis* sequences and Bld_BLi03393 one.

Fig. 2. UV-vis absorption spectra of YumC (A) and *R. palustris* FNR (B). Solid lines: air-oxidized, dotted lines: in the presence of 10-fold excess amount of NADPH, and broken lines: in the presence of excess (~ 20 fold) amount of dithionite. Measurements were performed at 25 °C under anaerobic conditions after several cycles of pure argon gas purging and evacuation. The mixture (2 ml) contained 18 μM of YumC or 14 μM of *R. palustris* FNR in 100 mM potassium phosphate buffer (pH 7.0).

Fig. 3. Difference spectra induced by addition of $NADP^+$ and/or Fd. (A): 18 μM YumC and (B): 15 μM *R. palustris* FNR, at 25 °C in 100 mM potassium phosphate buffer (pH 7.0). (A) **a** (dotted line): + 1 mM $NADP^+$, **b** (broken line): + 20 μM *B. subtilis* Fd, **c** (solid line): + 20 μM Fd and + 1 mM $NADP^+$, **d** (thin solid line): calculated spectrum, **a** + **b**, (B) **a** (dotted line): + 1 mM $NADP^+$; **b** (broken line): + 20 μM *B. subtilis* Fd, **c** (solid line): + 20 μM Fd and + 1 mM $NADP^+$, **d** (thin solid line): calculated spectrum, **a** + **b**. (C) Relationship between the magnitude of spectral change and $NADP^+$ concentration. YumC (○): $\Delta\varepsilon_{507}$ - $\Delta\varepsilon_{484}$, and *R. palustris* FNR (■): $\Delta\varepsilon_{506}$ - $\Delta\varepsilon_{481}$. Each 1–10 μl of $NADP^+$ (0.01 – 100 mM) stock solutions were added to the cuvettes containing 2 ml of 15 μM YumC or 16 μM *R. palustris* FNR solutions in 100 mM potassium phosphate buffer (pH 7.0) for the sample cell and 100 mM potassium phosphate buffer only for the reference cell. (D) Relationship between the magnitude of spectral change and *B. subtilis* Fd concentration. YumC (○): $\Delta\varepsilon_{382}$ - $\Delta\varepsilon_{404}$ and *R. palustris* FNR (■): $\Delta\varepsilon_{381}$ - $\Delta\varepsilon_{398}$. Each 1–10 μl of Fd (1.22 mM) stock solutions were added to the cuvettes containing 2 ml of 15 μM YumC or 16 μM *R. palustris* FNR solutions in 100 mM potassium phosphate buffer (pH 7.0) for the sample cell and 100 mM potassium phosphate

buffer only for the reference cell.

Fig. 4. Effects of NADPH concentration on the cytochrome *c* reduction activities of YumC (○) and *R. palustris* FNR (■). Assays were performed in 100 mM potassium phosphate buffer (pH 7.0) at 25 °C. Reaction mixtures contained 5 mM G6P, 5 U/ml of G6PDH, and; 20 μM NADPH, 0.1 mM horse heart cytochrome *c*, 5 μM *B. subtilis* Fd and NADPH as indicated. Reaction was initiated by addition of FNR solution (final concentrations of 1-4 nM) and cytochrome *c* reduction was monitored at 550 nm.

Fig. 5. Arrhenius plot of NADPH-ferricyanide diaphorase activities of YumC (○) and *R. palustris* FNR (■), and NADPH-cytochrome *c* reduction activity of YumC (●). Reaction was performed in 100 mM potassium phosphate buffer (pH 7.0) containing 10 mM G6P, 5 U/ml of G6PDH and; 1 mM NADPH and 1 mM or 2.9 mM ferricyanide for diaphorase assay, or 0.02 mM NADPH, 0.1 mM horse heart cytochrome *c* and 10 μM Fd for cytochrome *c* reduction assay. Reaction was initiated by addition of FNR solutions (final concentrations of 2–10 nM).

Fig. 6. The double reciprocal plot of cytochrome *c* reduction by YumC rate vs. NADPH concentration at fixed *B. subtilis* Fd concentrations. *B. subtilis* Fd: 0.2 μM(■), 0.5 μM (▲), 1 μM (♦), 2 μM (∗) and 5 μM (×). Each data point is the average of 4 or 5 independent measurements performed at 25 °C. Linear lines were obtained by fitting the data obtained at 0.1–2 μM NADPH at each Fd concentrations. The reaction mixture in 100 mM potassium phosphate buffer (pH 7.0) contained 0.1 mM cytochrome *c* from horse heart, 5 mM G6P, 5 U /ml of G6PDH, 1–4 nM YumC and indicated concentrations of Fd and NADPH.

Table 1

| | *B. subtilis* FNR (YumC) | *R. palustris* FNR (RPA3954) |
|---|---|---|
| **Diaphorase activity with ferricyanide** | | |
| $K_m$ (NADPH) | 10.9 ± 0.2[a] μM | 45 ± 3[a] μM |
| $k_{cat}$ ($s^{-1}$) | 900 ± 40[a] $s^{-1}$ | 346 ± 7[a] $s^{-1}$ |
| **Cytochrome *c* reductase activity with *B. subtilis* Fd** | | |
| $K_m$ (NADPH) | 0.19 ± 0.04[b] μM | ND[c] |
| $K_m$(Fd) | 2.7 ± 0.3[b] μM | > 5 μM |
| $k_{cat}$ ($s^{-1}$) | 99 ± 6[b] $s^{-1}$ | (4.62 ± 0.02[d] $s^{-1}$) |
| **Spinach Fd (at 10 μM)** | | |
| $k_{obs}$ ($s^{-1}$) | 0.172 ± 0.008 $s^{-1}$ | 0.068 ± 0.007 $s^{-1}$ |
| **RPA3956 (at 10 μM)** | | |
| $k_{obs}$ ($s^{-1}$) | 0.069 ± 0.004 $s^{-1}$ | 0.071 ± 0.008 $s^{-1}$ |
| **Direct cytochrome *c* reduction** | | |
| $k_{obs}$ ($s^{-1}$) | 0.057 ± 0.003 $s^{-1}$ | 0.068 ± 0.004 $s^{-1}$ |
| **NADPH oxidase (at 0.15 mM)** | | |
| $k_{obs}$ ($s^{-1}$) | 0.13[e] $s^{-1}$ | 0.027 ± 0.008 $s^{-1}$ |
| **NADH oxidase (at 0.15 mM)** | | |
| $k_{obs}$ ($s^{-1}$) | 0.58[e] $s^{-1}$ | 0.018 ± 0.007 $s^{-1}$ |
| $K_d$ for $NADP^+$ | 14 ± 3[f] μM | 41 ± 4[f] μM |
| $K_d$ for *B. subtilis* Fd | 1.7 ± 0.3[g] μM | 30 ± 5[g] μM |

a: In the presence of almost saturated concentrations of ferricyanide (3 mM for YumC and 1 mM for *R. palustris* FNR) and 0-1 mM NADPH.

b: Obtained with Eq.1 with data in Fig. 6.

c: $K_m$ value could not be determined because of strong substrate inhibition.

d: $k_{obs}$ at 10 μM *B. subtilis* Fd and 20 μM NADPH.

e: From ref [6].

f: Obtained with data in Fig. 3C.

g: Obtained with data in Fig. 3D.

Figure 1

A

```
bsu_BG12391      310 (gta)caaatgaagaaacccactactctaaaacggtcatgc(ata) 351
This work        310 (gta)acaaatgaagaaacccactactctaaaacggtcatc(ata) 351
```

B

```
bsu_BG12391       49 GVFKLVQMKKPTTLKRSCITAGNGAFKPRKLELENAEQYEGKNLHYFVDD 148
This work         49 GVFKLVTNEETHYSKTVIITAGNGAFKPRKLELENAEQYEGKNLHYFVDD 148
------------------------------------------------------------------------
consensus seq.                TNK--HYSK-VI
bld_BLi03393      49 GIFKLVTNKEIHYSKTVIITAGNGAFQPRKLELESAAQFENANLHYFIDD 148
bli_BL03143       49 GIFKLVTNKEIHYSKTVIITAGNGAFQPRKLELESAAQFENANLHYFIDD 148
bce_BC4926        51 GIFKLVTNKQTHYSKSVIITAGNGAFQPRRLELEGTAKYEKKNLHYFVDD 150
baa_BA_0033       49 GIFKLVTNKQTHYSKSVIITAGNGAFQPRRLELEGTAKYEKKNLHYFVDD 148
```

**Figure 2A**

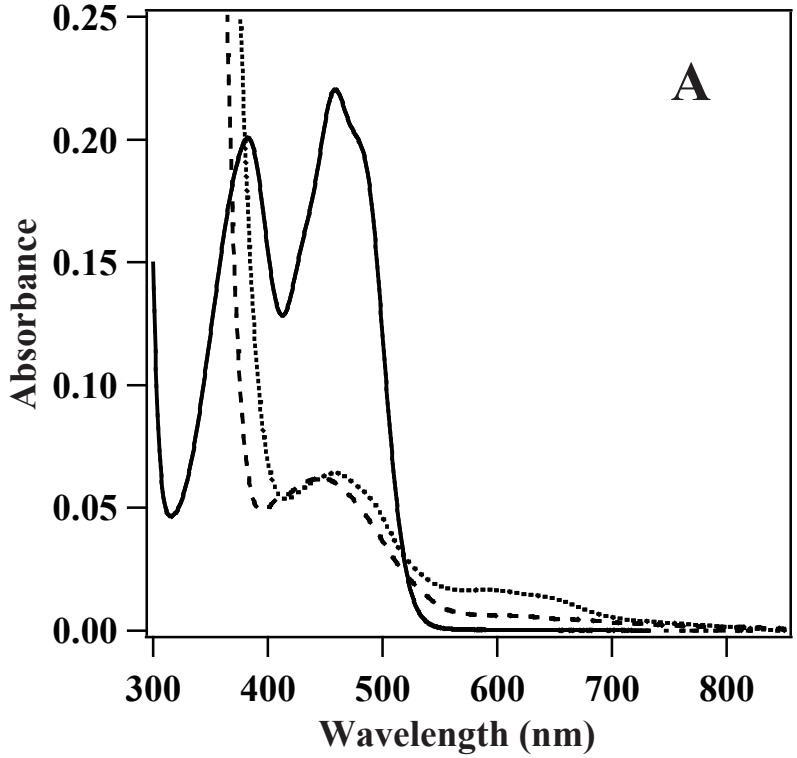
A
0.25
0.20
0.15
0.10
0.05
0.00
Absorbance
300
400
500
600
700
800
Wavelength (nm)

Figure 2B

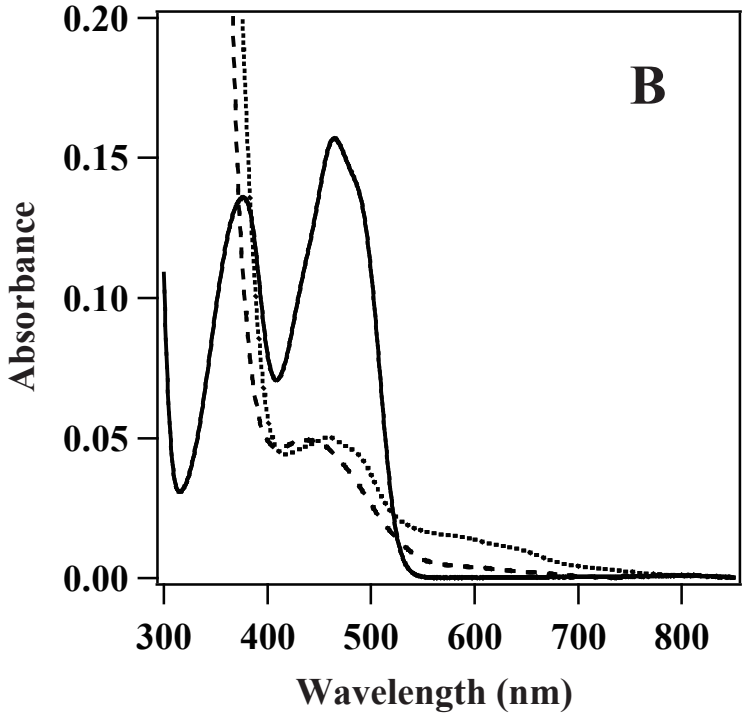
B
0.20
0.15
0.10
0.05
0.00
Absorbance
300
400
500
600
700
800
Wavelength (nm)

**Figure 3A**

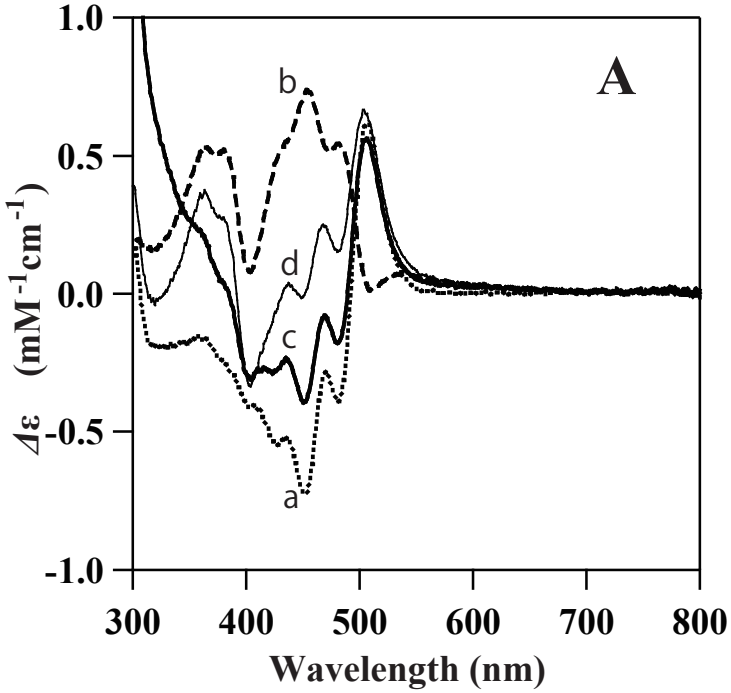
A
b
d
c
a
1.0
0.5
0.0
-0.5
-1.0
Δε (mM-1cm-1)
300
400
500
600
700
800
Wavelength (nm)

Figure 3B

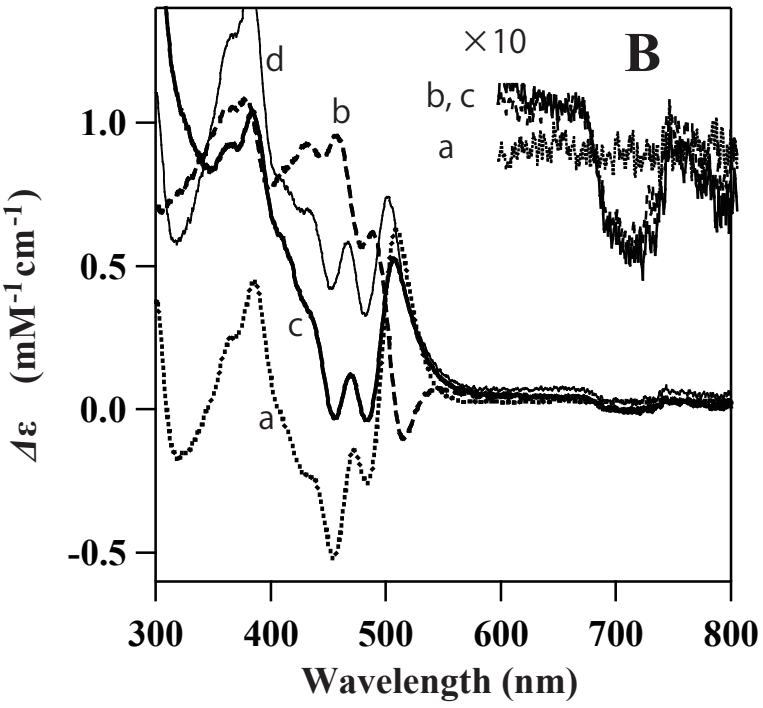
B
×10
b, c
a
d
b
c
a
1.0
0.5
0.0
-0.5
Δε (mM-1cm-1)
300
400
500
600
700
800
Wavelength (nm)

Figure 3C

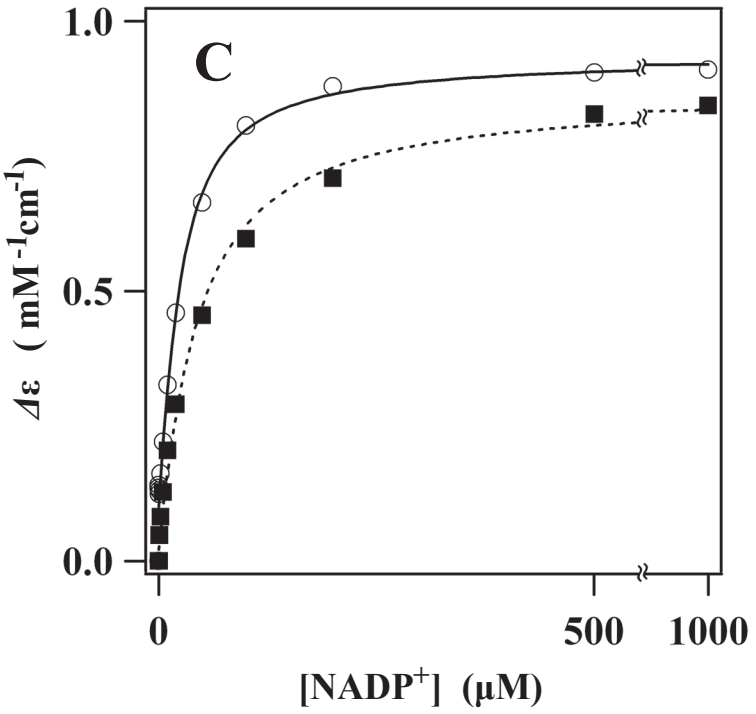

Figure 3D

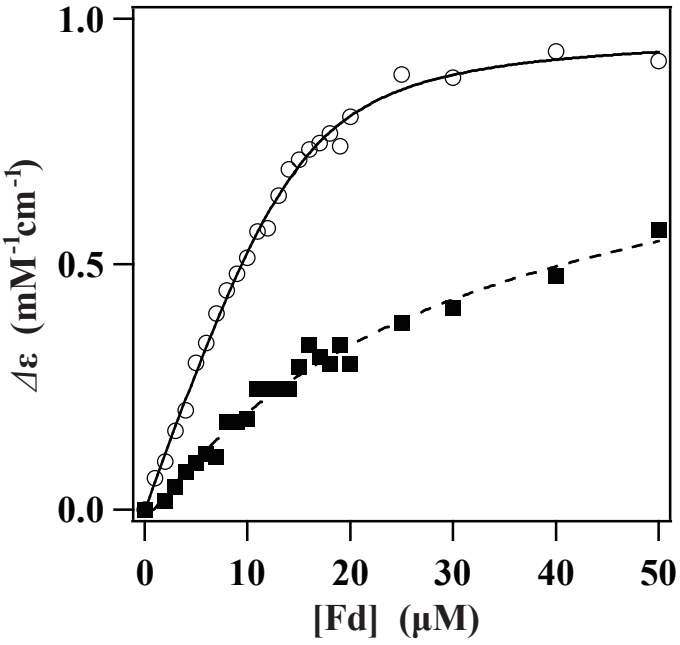

Figure 4

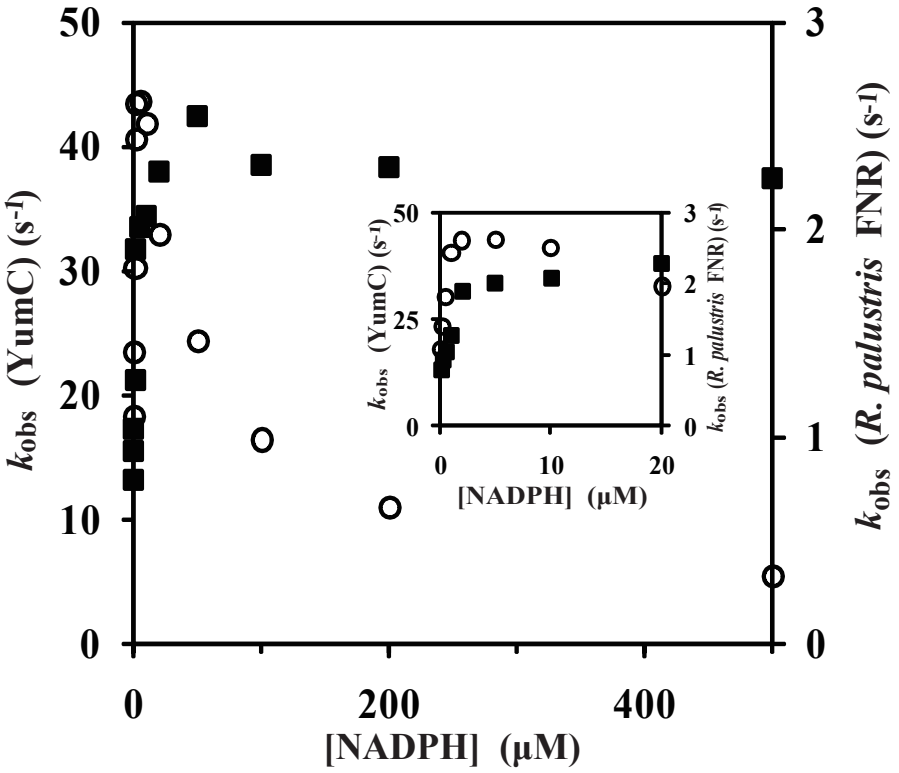
50
40
30
20
10
0
3
2
1
0
0
200
400
[NADPH] (µM)
$k_{obs}$ (YumC) ($s^{-1}$)
$k_{obs}$ (*R. palustris* FNR) ($s^{-1}$)
50
25
0
3
2
1
0
0
10
20
[NADPH] (µM)
$k_{obs}$ (YumC) ($s^{-1}$)
$k_{obs}$ (*R. palustris* FNR) ($s^{-1}$)

Figure 6

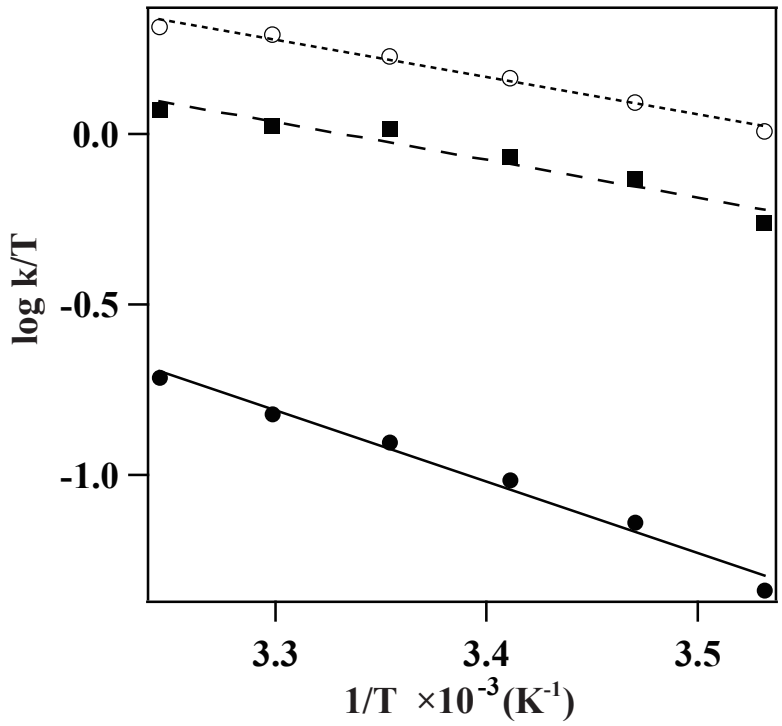

Figure 6